Analysis of Radar Observations of a Randomized Cloud Seeding Experiment

A. S. DENNIS, ALEXANDER KOSCIELSKI, D. E. CAIN, J. H. HIRSCH AND P. L. SMITH, JR.

Institute of Atmospheric Sciences, South Dakota School of Mines and Technology, Rapid City 57701

(Manuscript received 30 September 1974, in revised form 9 April 1975)

ABSTRACT

Magnetic tape records for radar observations of 80 moving one-hour test cases in a three-way randomized (no-seed, salt, silver iodide) cloud seeding experiment have been analyzed in terms of echoing areas and radar-estimated rainfall amounts. Individual test cases ranged from non-precipitating cumulus up to moderate thunderstorms with echoing areas exceeding 100 km^2 and rainfall estimated at 3000 kT in 1 h.

Out of numerous predictor variables, cloud depth is found to be the best single predictor for both echoing area and radar-estimated rainfall. The echoing area and radar-estimated rainfall are very closely correlated. A cube-root transformation of the radar-estimated rainfall improves the correlation between cloud depth and the radar-estimated rainfall for the no-seed (control) sample to 0.91. For clouds of a given depth, both the echoing area and radar-estimated rainfall are larger in seeded than in unseeded cases. The differences between no-seed and salt cases are of marginal statistical significance, but the differences in echoing area and rainfall between no-seed and silver iodide cases are significant at the 1% level. The indicated effects, expressed as a percentage of the echoing area or radar-estimated rainfall in the no-seed cases, decrease with cloud depth.

A comparison of no-seed and AgI cases with the aid of a one-dimensional steady-state cloud model shows that AgI seeding may have led to increases in maximum cloud height averaging 600 m.

It is concluded that seeding affected the precipitation in the Cloud Catcher test cases through both the microphysical processes and the cloud dynamics.

1. Introduction

Seeding of convective clouds can modify precipitation through both microphysical effects and alterations of cloud dynamics. As noted by many authors (e.g., Houghton, 1968) speeding the formation of precipitation in a convective cloud should increase its precipitation efficiency and lead to increases in rainfall even though the amount of water vapor entering the cloud remains unchanged. However, because of the overriding importance of cloud size in determining the total rainfall from a shower, a combination of microphysical and dynamic effects could change rainfall more radically than would microphysical effects alone. The most commonly sought dynamic effect is an increase in cloud height brought about by artificial glaciation of supercooled cloud water (e.g., Simpson and Dennis, 1974).

This paper presents an analysis of radar data from a randomized experiment on convective clouds designed to provide evidence concerning both microphysical and dynamic seeding effects. The possiblities that seeding of newly developing convective cloud towers is associated with changes in the horizontal extent, the height, and the rainfall production of the ensuing showers are investigated with the aid of standard statistical techniques and of a steady-state, one-dimensional cloud model.

2. Recording and reduction of radar data

a. Project design

The radar data which form the basis for this study were recorded on magnetic tape in 1969 and 1970 during Project Cloud Catcher, which was operated from about 1 June to 15 August both years from a radar facility 6 mi east of Rapid City. The project utilized moving target areas to follow developments within groups of convective clouds designated as test cases. By definition, each test case lasted 1 h from the time of its declaration.

A three-way randomization was used to permit testing of two seeding treatments, salt (powdered NaCl) and AgI. It was hypothesized that large cloud droplets of 50–100 μm diameter forming around salt particles could act as precipitation embryos (Biswas and Dennis, 1972), and that silver iodide seeding at the prescribed rates would release sufficient latent heat to stimulate cloud development. All seeding was carried out from an aircraft in updrafts below cloud base under control of the project meteorologist (Koscielski), who followed developments from the ground visually and on radar displays.

Test cases were declared by the project meteorologist after consultation with the crew of the seeding aircraft. Distinct clusters of cumulus clouds, well away from other showers, with updrafts of at least 2 m s^{-1} below cloud base and cloud top temperatures less than -10°C

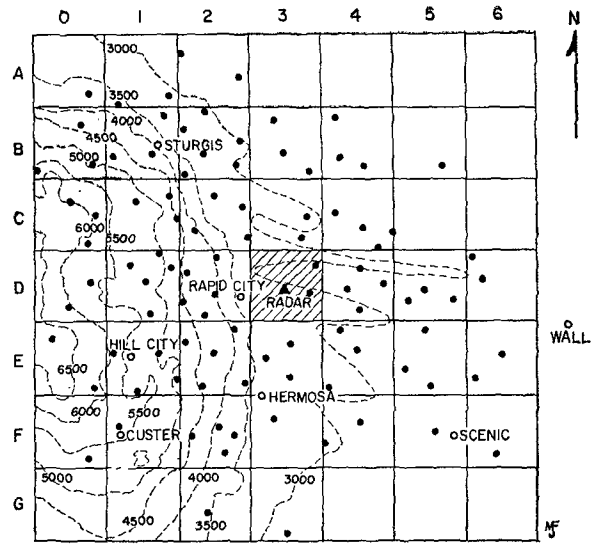

FIG. 1. Grid used to define Cloud Catcher test cases in 1969–70. Data were not collected from square D-3. Dashed lines are elevation contours in feet; heavy dots show location of raingages.

were selected as test cases. The existence of a radar echo did not prevent the selection of a cluster of growing clouds as a test case.

When a test case was declared, the crew of the seeding aircraft opened an envelope with the random instructions for that case. The allocation of instructions was AgI-seed ($\frac{1}{3}$), salt-seed ($\frac{1}{3}$), AgI-no seed ($\frac{1}{6}$), and salt-no seed ($\frac{1}{6}$). The crew then informed the project meteorologist of the selected treatment (AgI or salt), but did not tell him whether it was a seed or no-seed case. The seeding aircraft remained on station during no-seed cases and responded to all instructions except that no seeding agents were dispensed. For purposes of analysis, the AgI no-seed and salt no-seed cases are grouped in a single no-seed class involving (ideally) one-third of all the cases. In 1970 the procedure was changed in that the random choice for the first test case of the day was applied to subsequent cases, if any, to reduce the chances of contamination.

Salt seeding was carried out by releasing up to 50 kg of powdered NaCl in updrafts below cloud base. Silver iodide seeding was accomplished by burning flares containing 120 g AgI each in the updrafts, with up to six flares used on the largest cases. Elementary calculations regarding the resultant particle concentrations in the clouds have been given by Dennis and Koscielski (1972) and (for salt only) by Biswas and Dennis (1972).

Additional information on the operation of the project and individual test cases is provided by Dennis *et al.* (1974).

b. *Radar data recording*

Data from a modified Nike-Ajax X-band radar were fed to an on-line minicomputer which calculated equivalent radar reflectivity factors (Z_e) and recorded them on magnetic tape. The radar antenna provided a 1.2° conical beam. Radar data were logged in Cartesian coordinates with horizontal resolution of 0.5 n mi at eight heights beginning at 10,000 ft[1] and continuing in 5000 ft increments to 45,000 ft. Test cases were defined in terms of a fixed grid of squares each 10 n mi on a side extending to 35 n mi from the radar site (Fig. 1). The test cases moved through the grid, usually occupying two squares at any moment. On a few occasions, when test cases straddled a line or an intersection of the grid system, data were logged from three or even four squares. Logging the radar data from two squares took from 5 to 8 min depending upon the range of the test case from the radar. The data logging system has been described in detail by Smith (Dennis *et al.*, 1974, Appendix B).

c. *Radar data reduction*

The present analysis deals with echoes at the 10,000 ft level. This was the lowest height from which data could be recorded without interruption by the Black Hills, some of which surpass 7000 ft in altitude, in the western part of the experimental area. As it happened, the average cloud base height for the test cases of the two summers was near 10,000 ft, so the analysis can be considered as a study of cloud base events.

Echoing areas within test case squares with values of $Z_e > 30$ dBZ have been tabulated and averaged over the lifetime of each case. The mean echoing area is denoted henceforth by A30. The tabulation of echoing areas exceeding a fixed threshold of Z_e rather than the total area with detectable echoes reduces variations with range which might bias the results. Initial echoing areas exceeding 30 dBZ (denoted by $A30_i$) have also been calculated for each case along with other radar parameters used in the statistical evaluation. Further discussion of these is deferred until Section 3d.

Radar rainfall rates have been calculated from the Marshall-Palmer relationship

$$Z_e = 200\, R^{1.6},$$

where Z_e is expressed in $mm^6\ m^{-3}$ and R is rainfall rate ($mm\ h^{-1}$). The radar rainfall rates have been integrated in space and time by a computer to yield preliminary estimates of rainfall for each test case.

The preliminary computer estimates were usually accepted as final values of RER, the radar-estimated rainfall. Sometimes adjustments were made, such as by rejecting data from a scan when interference caused spurious signals to appear in the radar echo integrator. A difficulty arose for some test cases of 1969, when the experimental design required the project meteorologist to specify at the time of test case declaration the squares from which radar data would be logged. Adjustments were made on the basis of auxiliary radar and raingage data for those test cases which extended outside of the

[1] All heights MSL unless noted.

squares specified for data logging by the minicomputer. Such adjustments were not needed in 1970, when the meteorologist was not required to specify in advance the squares from which radar data would be recorded.

The rainfall estimates are necessarily crude due to 1) attenuation, 2) evaporation between cloud base and the ground, and 3) the application of a Z-R relationship derived in eastern Canada to showers in the northern Great Plains, some of which contained hail. The last two sources of error would generally cause overestimates of rainfall at the ground and so compensate in part for attenuation, which causes underestimates. Lacking a satisfactory means of correcting for attenuation, we feel that it would imply an unreal degree of precision to attempt to improve upon the Marshall-Palmer formula for X-band radar data.

d. Comparison with raingage data

A check on the accuracy of the rainfall estimates was provided by a network of conventional raingages in the project area which were read at 0900 and 2100 MDT each day by volunteer observers (Fig. 1). The radar rainfall estimates were compared with estimates based upon the raingage observations for four large test cases (Table 1). These were the only cases for which comparisons were possible. On other test case days some of the rainfall measured by the gages fell from cells unrelated to the experiment and prevented any meaningful comparison with the radar data. The raingage readings were plotted and analyzed by hand with the aid of time lapse radar photographs. An example appears as Fig. 2.

There is fair agreement between the rainfall estimates from the radar-computer system and those from the isohyetal analysis (Table 1). The overestimate of rainfall for Case 70-15A may be due to the considerable amount of small hail noted in it. As the value of RER in the Cloud Catcher cases which actually rained ranged over several orders of magnitude, from a few kilotons for a small shower to several thousand kilotons for a sizable thunderstorm, the uncertainties of 10% to 50% suggested by Table 1 do not preclude meaningful analyses in terms of rainfall production per case.

TABLE 1. Comparison of radar-estimated rainfall (RER) with results of isohyetal analysis. X-band radar: $Z_e = 200\ R^{1.6}$

Case number	Date	RER (kT)*	Estimate from isohyetal analysis (kT)	Number of gages with rain
70-1A (no-seed)	6/08/70	1300	1200	5
70-15A (no-seed)	7/28/70	1000	640	3
70-21 and 70-21A (AgI)	8/11/70	5200	5900	11

* 1 kiloton (kT) = 1000 metric tons = 10^9 g.

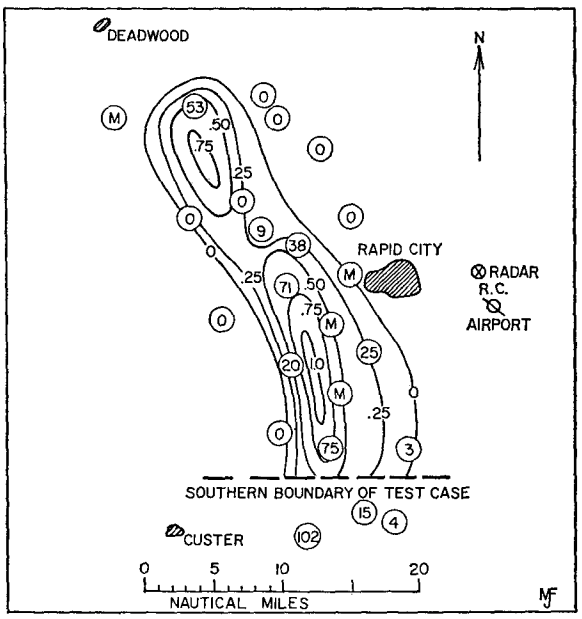

FIG. 2. Isohyetal map for Cases 70-21 and 70-21A on 11 August 1970 based on rainfall observations for period 0900–2100 MDT and time lapse photographs of PPI radar display. Plotted amounts are in hundredths of an inch. Estimate from map is 5900 kT compared to radar-estimated rainfall (RER) of 5200 kT.

e. First comparison of no-seed, salt, and silver iodide cases

A simple comparison of the mean echoing area and the radar-estimated rainfall for the no-seed, salt, and silver iodide cases is given in Table 2. The average rainfall per salt case is equal to the average rainfall per no-seed case (370 kT), while the average rainfall per silver iodide case is greater at 440 kT. Because of the highly skewed distribution of rainfall amounts the averages are strongly influenced by the few largest cases in each class. A rank-sum test does not show any significant differences among the three classes.

TABLE 2. Mean echoing area and radar-estimated rainfall for no-seed, salt, and silver iodide cases.

		Mean echoing area (A30)		Radar-estimated rainfall	
	Number of cases	Average (km^2)	Standard deviation (km^2)	Average (kT)	Standard deviation (kT)
No-seed	33	38	47	370	470
Salt	29	44	66	370	560
Silver iodide	18	41	70	440	920

TABLE 3. Summary statistics for 33 no-seed cases.

Variable		Mean	Standard deviation	Correlations* PWA	CBH	CBT	MEH	CDP	RUP	WMX	HWM	TWM	FEH	FET	$(A30_i)^{\frac{1}{3}}$	$(A30)^{\frac{1}{3}}$	$(RER)^{\frac{1}{3}}$
Precipitable water (mm)	PWA	24.1	5.9		−0.11	0.50	0.27	0.29	−0.05	0.17	0.21	−0.04	−0.04	0.40	−0.21	0.20	0.12
Cloud base height (km)	CBH	2.9	0.4			−0.65	0.09	−0.07	−0.20	−0.22	0.35	−0.39	−0.19	0.07	0.13	−0.01	0.00
Cloud base temperature (°C)	CBT	11.0	3.6				0.14	0.24	0.04	0.52	0.00	0.19	0.20	0.09	−0.16	0.11	0.10
Maximum echo height (km)	MEH	9.4	2.4					0.99	0.40	0.69	0.77	−0.70	0.21	−0.13	0.44	0.90	0.91
Cloud depth (km)	CDP	6.5	2.4						0.43	0.73	0.71	−0.64	0.24	−0.14	0.42	0.90	0.91
Radius of updraft (km)	RUP	1.4	0.7							0.59	0.10	−0.04	0.45	−0.34	0.33	0.54	0.56
Maximum updraft velocity (m s^{-1})	WMX	16.5	6.4								0.42	−0.28	0.04	−0.29	0.36	0.66	0.71
Height of WMX (km)	HWM	6.7	1.9									−0.97	0.07	−0.40	0.25	0.63	0.62
Temperature of WMX (°C)	TWM	−14.5	13.0										−0.03	0.09	−0.27	−0.57	−0.57
Average first echo height (km above CBH)	FEH	3.3	0.8											−0.79	0.01	0.22	0.21
Average first echo temperature (°C)	FET	−14.8	5.8												−0.16	−0.12	−0.16
Initial echo area with $Z_e>30$ dBZ† ($km^{\frac{1}{3}}$)	$(A30_i)^{\frac{1}{3}}$	1.4	1.8													0.56	0.60
Average echo area with $Z_e>30$ dBZ† ($km^{\frac{1}{3}}$)	$(A30)^{\frac{1}{3}}$	2.4	1.9														0.97
Radar estimated rainfall ($kT^{\frac{1}{3}}$)	$(RER)^{\frac{1}{3}}$	5.3	3.8														

* Correlations of 0.35 or greater absolute value are significant at the 5% level.
† Cube-root transformation applied.

3. Statistical analysis

a. Selection of predictors

As noted above, the Cloud Catcher test cases covered a wide size range. This range was deliberately sought as an aid in investigation of factors influencing the rainfall from a convective cloud.

Data were collected by a number of sensors not mentioned so far, including time lapse cloud cameras and, during 1970, by a cloud physics aircraft. However, we tried to limit the selection of predictors of shower extent and total test case rainfall to variables which could be defined objectively for each case. This ruled out the data from the instrumented aircraft, for example, which was not only incomplete but biased toward the weaker clouds in some test cases because of safety considerations.

Of the twelve predictors selected, only those dealing with first echoes have any missing data. Most of the time this was due to the complete absence of first echoes. Two salt cases of 1969 lack 3 cm radar data and have been dropped from the analysis of horizontal shower extent; rainfall for these two cases was estimated from other radar data.

b. Observed predictors

The precipitable water (PWA) is defined as the precipitable water from the surface to 500 mb on the Rapid City rawinsonde observation at 1700 MST. The cloud base height (CBH) was determined by the crew of the seeding aircraft operating below cloud base. The cloud base temperature (CBT) was determined by comparing the reported value of CBH to the plotted rawinsonde information.

The radar observations usually yielded a maximum echo height (MEH), with the cloud depth (CDP) being obtained by subtracting CBH from MEH. For cases without radar echoes, the maximum cloud top was estimated from time lapse cloud photographs and used for MEH.

The radius of updraft (RUP) was estimated by the project meteorologist after viewing time lapse pictures of the test case clouds and of a PPI radar display and examining notes taken by the observer on the cloud seeding aircraft and by the observer on the instrumented aircraft, which was used to probe some of the cases near the $-10°$C level. The meteorologist's objective was to estimate the value of RUP at the time of strongest convective activity in the test case. As the updrafts were erratic and irregularly shaped, the values of RUP are only approximate.

c. Cloud model predictors

A modified version of a one-dimensional, steady-state cloud model developed at Pennsylvania State University (e.g. Weinstein and MacCready, 1969) was run with the 1700 MST rawinsonde data and the estimated updraft radius to yield a predicted updraft profile for each test case (Hirsch, 1972). This profile provided the maximum updraft velocity (WMX), the height at which the maximum updraft occurred (HWM), and the temperature at the level of maximum updraft (TWM). Each model run used the appropriate version of the cloud model for the test case under consideration (i.e., AgI version for AgI cases, salt version for salt cases, natural version for no-seed cases). Comments on the validity of the model are given in Section 4.

d. Radar-derived predictors

In addition to the maximum echo height (MEH), three other predictors were drived from the taped radar data. Average first echo height (FEH) and the average first echo temperature (FET) were previously derived and analyzed by Dennis and Koscielski (1972). They are included here, with the average values used for those cases without identifiable first echoes.

In view of the tendency for large showers to persist longer than small ones, the extent of radar echo at the time of test case declaration appears as a possible predictor of A30 and RER. The area with $Z_e > 30$ dBZ on the initial scan, denoted by $A30_i$, has been determined for those cases with good scans close to the time of test case declaration.

e. Preliminary look at statistics

Summary statistics for the no-seed, salt, and silver iodide cases are listed in Tables 3, 4 and 5 respectively. Cube-root transformations have been applied to A30, $A30_i$ and RER to improve the correlation coefficients, as noted below. The correlations involving FEH and FET have been calculated inserting mean values for cases without identifiable first echoes and so are slightly different from those of Dennis and Koscielski (1972).

The radar-estimated rainfall (RER) is seen to be so closely correlated with the mean echoing area (A30) as to suggest that a good estimate of RER could be obtained merely by noting the value of A30.

The random selection process failed to yield an unbiased selection of no-seed, salt, and silver iodide cases. There are differences among the three classes not related to possible seeding effects. A rank-sum test shows differences between the no-seed and salt classes in PWA at the 0.11 (two-tailed) significance level, in CBH at the 0.01 significance level, and in CBT at the 0.05 significance level. The same test shows differences between the no-seed and silver iodide cases in CBH (0.002 level) and CBT (0.005 level).

The significant differences in conditions in the subcloud layer between the no-seed and seed cases confirm the need for predictors for A30 and RER.

TABLE 4. Summary statistics for 29 salt cases.

Variable		Mean	Standard deviation	Correlations* PWA	CBH	CBT	MEH	CDP	RUP	WMX	HWM	TWM	FEH	FET	$(A30_i)^{\frac{1}{3}}$	$(A30)^{\frac{1}{3}}$	$(RER)^{\frac{1}{3}}$
Precipitable water (mm)	PWA	21.1	6.0		−0.38	0.49	0.57	0.64	0.51	0.27	0.19	0.04	0.12	0.18	0.35	0.34	0.36
Cloud base height (km)	CBH	3.2	0.5			−0.62	0.12	−0.06	0.14	0.01	0.14	−0.17	−0.06	−0.24	0.06	0.12	0.06
Cloud base temperature (°C)	CBT	9.0	4.5				0.13	0.24	0.01	0.44	0.30	−0.01	0.12	0.12	0.14	0.14	0.11
Maximum echo height (km)	MEH	8.9	2.4					0.98	0.78	0.65	0.58	−0.43	0.05	0.08	0.69	0.86	0.86
Cloud depth (km)	CDP	5.8	2.4						0.76	0.65	0.55	−0.40	0.07	0.12	0.68	0.85	0.85
Radius of updraft (km)	RUP	1.2	0.6							0.64	0.46	−0.35	0.14	−0.05	0.55	0.63	0.66
Maximum updraft velocity (m s^{-1})	WMX	13.8	6.0								0.66	−0.46	0.10	−0.03	0.58	0.66	0.67
Height of WMX (km)	HWM	6.1	1.5									−0.92	0.07	−0.09	0.49	0.45	0.45
Temperature of WMX (°C)	TWM	−10.2	8.6										−0.02	0.10	−0.37	−0.30	−0.34
Average first echo height (km above CBH)	FEH	1.6	1.0											−0.90	0.20	0.06	0.11
Average first echo temperature (°C)	FET	−3.1	8.2												−0.13	0.05	0.01
Initial echo area with $Z_e>30$ dBZ† ($km^{\frac{1}{3}}$)	$(A30_i)^{\frac{1}{3}}$	1.6	2.1													0.80	0.80
Average echo area with $Z_e>30$ dBZ† ($km^{\frac{1}{3}}$)	$(A30)^{\frac{1}{3}}$	2.5	2.0														0.99
Radar estimated rainfall ($kT^{\frac{1}{3}}$)	$(RER)^{\frac{1}{3}}$	5.1	3.9														

* Correlations of 0.37 or greater absolute value are significant at the 5% level.
† Cube-root transformation applied.

TABLE 5. *Summary statistics for 18 silver iodide cases.*

Variable		Mean	Standard deviation	Correlations* PWA	CBH	CBT	MEH	CDP	RUP	WMX	HWM	TWM	FEH	FET	$(A30_i)^{\frac{1}{3}}$	$(A30)^{\frac{1}{3}}$	$(RER)^{\frac{1}{3}}$
Precipitable water (mm)	PWA	22.2	3.9		−0.15	0.12	0.11	0.13	0.13	−0.11	0.01	0.05	0.12	−0.08	0.13	−0.13	−0.11
Cloud base height (km)	CBH	3.3	0.5			−0.85	−0.07	−0.26	−0.17	−0.37	−0.13	0.08	−0.61	0.34	0.11	−0.27	−0.38
Cloud base temperature (°C)	CBT	8.5	3.9				0.30	0.45	0.31	0.63	0.29	−0.16	0.73	−0.50	−0.12	0.35	0.49
Maximum echo height (km)	MEH	8.6	2.4					0.98	0.71	0.81	0.76	−0.66	0.46	−0.50	0.48	0.82	0.80
Cloud depth (km)	CDP	5.2	2.4						0.73	0.86	0.76	−0.66	0.56	−0.55	0.45	0.85	0.85
Radius of updraft (km)	RUP	1.2	0.7							0.73	0.72	−0.62	0.38	−0.36	0.21	0.74	0.72
Maximum updraft velocity ($m\ s^{-1}$)	WMX	14.5	7.3								0.86	−0.77	0.54	−0.46	0.28	0.79	0.83
Height of WMX (km)	HWM	6.5	2.0									−0.98	0.18	−0.18	0.35	0.69	0.66
Temperature of WMX (°C)	TWM	−11.9	12.5										−0.05	0.06	−0.37	−0.62	−0.57
Average first echo height (km above CBH)	FEH	2.1	1.2											−0.92	0.09	0.39	0.53
Average first echo temperature (°C)	FET	−7.4	7.2												−0.20	−0.37	−0.47
Initial echo area with $Z_e>30$ dBZ† ($km^{\frac{1}{3}}$)	$(A30_i)^{\frac{1}{3}}$	1.6	1.6													0.53	0.51
Average echo area with $Z_e>30$ dBZ† ($km^{\frac{1}{3}}$)	$(A30)^{\frac{1}{3}}$	2.4	1.9														0.97
Radar estimated rainfall ($kT^{\frac{1}{3}}$)	$(RER)^{\frac{1}{3}}$	5.0	4.1														

* Correlations of 0.47 or greater absolute value are significant at the 5% level.
† Cube-root transformation applied.

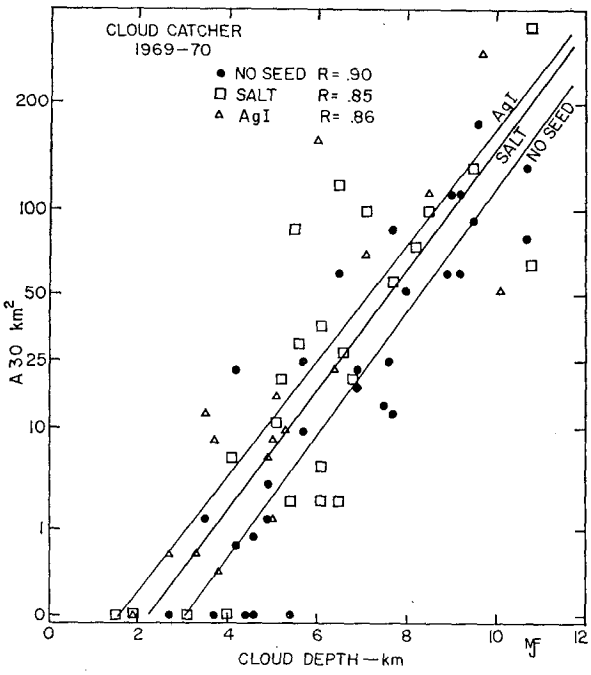

FIG. 3. Mean echoing area exceeding 30 dBZ (A30) vs cloud depth (CDP) for no-seed, salt, and silver iodide cases. A cube-root transformation has been applied to A30 to improve the correlation with CDP.

f. Mean echoing area and radar-estimated rainfall as functions of cloud depth

Correlations with non-transformed data showed CDP to be the best single predictor of A30 and RER for the no-seed cases. This suggested a covariance analysis of A30 and RER as functions of CDP.

It is well known that CDP is correlated with radius of updraft and updraft speed (e.g., Simpson and Dennis, 1974), and these correlations appear in the present data (Tables 3–5). CDP is also correlated with cloud lifetime, although the 1 h limit on Cloud Catcher test cases would reduce the impact of this correlation. The rainfall from a shower must be a product of these factors multiplied by some preciptation efficiency term. Therefore, RER should vary as some power of CDP or, to put it another way, some root of RER should show a greater linear correlation with CDP than does RER itself.

We have studied the correlation between $(\text{RER})^a$ and CDP for values of a ranging from 0.25 to 1.00 using a computer optimization program by Hooke and Jeeves (1961). Setting a at 0.321 maximizes the correlation coefficient for the no-seed sample at 0.91, as compared to 0.81 for the untransformed data. The cube-root transformation yields almost identical results, so it is used for the balance of this study. The hypothesis that the cube-root transformed rainfall estimates follow a normal distribution is not rejected by standard statistical tests.

It might seem strange that the cube-root transformation, which is sometimes applied to observations over several hours, would be optimum for 1 h test cases. However, RER refers to rainfall over an echoing area of up to 100 km², rather than at a point.

Optimization of the correlation coefficient between A30 and cloud depth (CDP) showed the correlation coefficient for the no-seed sample to be maximized, again at 0.91, by using the variable $(\text{A30})^{0.37}$. Once again, a cube-root transformation yielded almost the same results, so cube-root transformations have been applied to both A30 and A30_i.

The covariance analyses have been carried out under the assumption that all test cases were independent. Strong autocorrelation among test cases occurring on the same day could reduce the number of degrees of freedom in the analysis, particularly in 1970 when randomization was changed from case by case to a daily basis to permit the selection of successive test cases in the same part of the grid without risk of contamination. However, most days produced only one or two test cases and the multiple test cases occurring on the same day often varied widely. For example, the four no-seed cases on 28 July 1970, the day with the largest number of test cases, had tops (MEH) of 7.3, 12.2, 12.2 and 6.4 km in that order.

The covariance analysis of $(\text{A30})^{\frac{1}{3}}$ as a function of CDP is presented in Fig. 3, which shows the separate regression lines for the three classes of cases fitted by the least squares method. The significance levels are given in Table 6.

The difference in adjusted[2], transformed mean echoing area between the AgI and no-seed classes is significant at the 1% level. The difference in adjusted

TABLE 6. Results of covariance analysis of $(\text{A30})^{\frac{1}{3}}$ versus CDP for cases of 1969–70.

Class	Regression line*	Correlation
No-seed	$(\text{A30})^{\frac{1}{3}} = -2.15 + 0.70$ CDP	0.90
Salt	$(\text{A30})^{\frac{1}{3}} = -1.54 + 0.68$ CDP	0.85
AgI	$(\text{A30})^{\frac{1}{3}} = -1.05 + 0.66$ CDP	0.86

	Significance levels		
	No-seed vs salt	No-seed vs AgI	Salt vs AgI
Among means	0.04	<0.01	0.26
One line	0.12	0.01	0.53
Same slope	0.65	0.67	0.66

* A30 is in km², CDP in km.

[2] The mean echoing areas for the two classes are compared with an adjustment obtained by applying an estimated regression coefficient to the difference in the mean value of the independent variable (mean cloud depth) for the two classes (see Dixon and Massey, 1957, pp. 214–215).

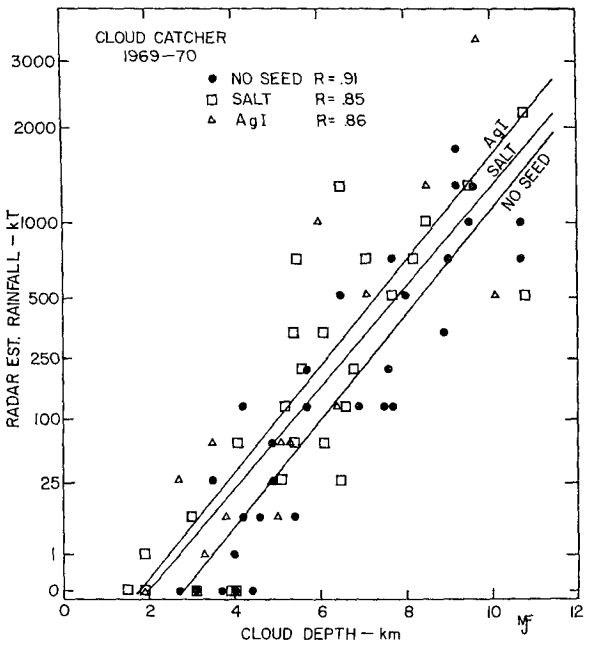

FIG. 4. Scatter diagram of the cube root of radar estimated rainfall, $(RER)^{\frac{1}{3}}$, vs cloud depth for no-seed, salt, and silver iodide cases.

means for the no-seed and salt classes is significant at the 4% level. The difference in adjusted means for the salt and AgI cases is not significant. There is no evidence of any differences in the slopes of the regression lines (Table 6).

The covariance analysis of $(RER)^{\frac{1}{3}}$ vs CDP (Fig. 4 and Table 7) shows practically the same pattern as the analysis of $(A30)^{\frac{1}{3}}$ vs CDP. This is not surprising in view of the strong correlation between $(RER)^{\frac{1}{3}}$ and $(A30)^{\frac{1}{3}}$ shown in Tables 3–5. The difference in adjusted means between the no-seed and AgI classes is significant at the 1% level, while the difference between the no-seed and salt classes is significant at the 6% level. The difference between the salt and silver iodide classes is not significant.

We conclude on the basis of the data displayed in Figs. 3 and 4 that the relationships between mean echoing area at cloud base and cloud depth were different for the seed and no-seed cases and that the relationships between radar-estimated rainfall and cloud depth were also different. Both salt and silver iodide are associated with large mean echoing areas and radar estimates of rainfall as compared to the no-seed cases in the same range of cloud depth.

The slopes of the regression lines in Figs. 3 and 4 are the same for all classes but, because of the data transformations, this similarity does not indicate a constant percentage difference in echoing area or radar-estimated rainfall among the three classes. Expressed as a percentage of the echoing area in the no-seed cases, the differences are most pronounced for the small clouds and decrease with increasing cloud depth. All clouds more than 2 km deep that were seeded with silver iodide produced radar echoes, while some unseeded and salt-seeded cases over 4 km deep failed to produce echoes.

TABLE 7. Results of covariance analysis of $(RER)^{\frac{1}{3}}$ versus CDP for cases of 1969–70.

Class	Regression equation*	Correlation
No-seed	$(RER)^{\frac{1}{3}} = -4.02 + 1.43$ CDP	0.91
Salt	$(RER)^{\frac{1}{3}} = -2.71 + 1.36$ CDP	0.85
AgI	$(RER)^{\frac{1}{3}} = -2.62 + 1.44$ CDP	0.87

	Significance levels		
	No-seed vs salt	No-seed vs AgI	Salt vs AgI
Among means	0.06	0.01	0.43
One line	0.17	0.03	0.67
Same slope	0.68	0.43	0.69

*RER is in kT, CDP in km.

In considering the possibility that the results of Table 7 imply rainfall increases due to seeding, it is necessary to consider the possibility that seeding changes drop size distributions. Raindrop size observations were not taken on Project Cloud Catcher. With regard to the effects of hygroscopic seeding, recent modeling studies indicate that the coalescence-breakup process leads to nearly the same raindrop size distribution at cloud base regardless of the size spectrum of the assumed raindrop embryo population (Farley and Chen, 1975). Observations of drop sizes at cloud base in Florida failed to show any significant differences between unseeded clouds and clouds seeded with silver iodide.[3] However, cloud bases in Florida are typically 4 km below the freezing level, compared to 2 km below the freezing level in western South Dakota.

The distributions of reflectivity factors (Z_e values) in the no-seed, salt, and silver iodide cases are shown in Fig. 5. The distributions of Z_e values for the three classes of cases are similar, with the highest values in the silver iodide cases. Fig. 5 implies that changes in Z_e due to changes in drop size, if any, are offset by changes in hydrometeor concentrations. Furthermore, the indicated seeding effect is *not* the addition of a tail of very light rain or virga to the natural rainfall rate distribution, but rather the addition of echoing areas resembling natural showers in intensity.

g. Search for refined predictions by MLR *techniques*

A multiple linear regression (MLR) analysis has been carried out for each of the three classes in an attempt to identify additional factors related to precipitation formation. The 5% significance level was used in determining whether or not additional predictors should be admitted to the MLR formulas.

[3] Private communication from J. Simpson.

The resultant formulas are as follows (units are as in Tables 3–5; the predictors are shown in the order of selection; the value of R, the multiple correlation coefficient, following each step in the selection process is shown):

No-seed:	$(A30)^{\frac{1}{3}}=0.59\ (CDP)+0.21\ (A30_i)^{\frac{1}{3}}+0.39\ (RUP)-2.24$				
	R: 0.904	0.925	0.934		
Salt:	$(A30)^{\frac{1}{3}}=0.47\ (MEH)+0.43\ (A30_i)^{\frac{1}{3}}-2.46$				
	R: 0.864	0.908			
AgI:	$(A30)^{\frac{1}{3}}=0.68\ (CDP)-0.12\ (PWA)+1.57$				
	R: 0.856	0.902			
No-seed:	$(RER)^{\frac{1}{3}}=1.17\ (CDP)+0.55\ (A30_i)^{\frac{1}{3}}+0.74\ (RUP)-4.11$				
	R: 0.911	0.944	0.953		
Salt:	$(RER)^{\frac{1}{3}}=1.27\ (MEH)+0.84\ (A30_i)^{\frac{1}{3}}-0.19\ (PWA)-0.14\ (CBH)+1.16$				
	R: 0.853	0.901	0.915	0.926	
AgI:	$(RER)^{\frac{1}{3}}=1.44\ (CDP)-2.62$				
	R: 0.866				

Although the MLR analysis yields additional "significant" predictors, it is difficult in some cases to see their physical significance. The results do suggest using initial echoing area as a predictor to take account of the persistence of cells existing at the time of test case declaration. We have found little impact thereby on the significance levels already quoted on the basis of the covariance analysis, so this approach will not be pursued further in this paper.

4. Further analysis of effects of silver iodide seeding with the aid of the cloud model

a. General

The work plans for Project Cloud Catcher called for a comparison of the heights achieved by no-seed and AgI seed cases in an attempt to detect dynamic effects. A simple comparison of the values of MEH for the no-seed and AgI classes is not an adequate test in view of the differences in CBH and CBT between the two classes. The tabulated variables CBH and RUP, plus the environmental soundings obtained by the rawinsonde released from Rapid City at 1700 MST each day, are sufficient input to define the steady-state cloud model for each case, providing predicted cloud tops for comparison with the radar observations.

b. Test of model

The model's performance was first tested by comparing the predicted cloud top with the observations of MEH for each of the 33 no-seed cases (Fig. 6). The resultant set of data is summarized under "no-seed cases" in Table 8; data for individual cases are given by Dennis *et al.* (1974). Obviously, visible cloud tops must exceed the true value of MEH by a few hundred meters at least, and Table 8 does show the predicted no-seed cloud top (NCT) to average slightly higher than the maximum echo height (MEH). However, beamwidth errors in MEH are comparable to this difference, and a simple t-test fails to reject the hypothesis that the means of MEH and NCT are equal.

The correlation coefficient between NCT and MEH of 0.89 is significant at the 1% level. It is similar to

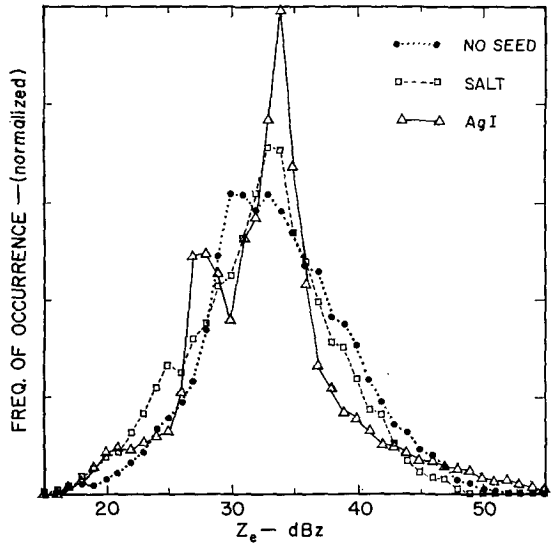

FIG. 5. Distribution of equivalent radar reflectivity factor (Z_e) at 10,000 ft MSL for the no-seed, salt, and silver iodide cases.

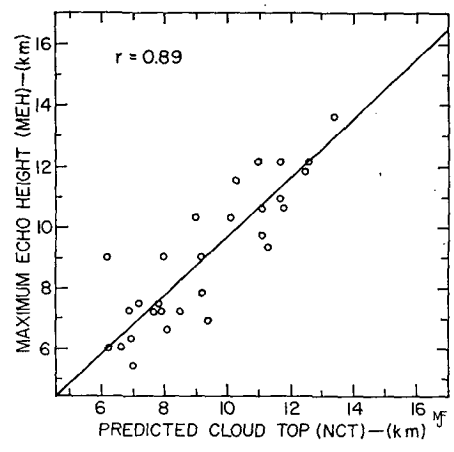

FIG. 6. Maximum echo height vs cloud top heights predicted by no-seed version of the model for 33 no-seed cases.

TABLE 8. Mean heights (km) for 33 no-seed cases and 18 AgI-seed cases from radar observations, no-seed model, and AgI model.

	No-seed cases	AgI cases
Maximum radar echo height (MEH)	9.38	8.56
No-seed model cloud top (NCT)	9.62	8.19
AgI model cloud top (ACT)	10.17	9.68

the 0.88 found by Weinstein and MacCready (1969) in Arizona. We conclude that the modified steady-state model is applicable to clouds of the northern Great Plains as far as height determinations are concerned.

c. Effects of AgI seeding on cloud height

The effect of AgI seeding upon cloud height is tested by comparing MEH−NCT for no-seed and AgI cases (Tables 8 and 9). The average difference between MEH and NCT is −230 m for the no-seed cases and 370 m for the AgI cases, suggesting average growth of 600 m due to seeding. A rank-sum test comparing MEH−NCT for the two classes yields a test statistic of 1.64, which is significant at the 10% level and therefore suggests that the 600 m apparent growth due to seeding is real. This is much smaller than the 1800 m average increase in height due to seeding noted by Weinstein and MacCready for clouds near Flagstaff.

d. Testing the AgI model

Silver iodide seeding was simulated by changing cloud water to cloud ice in a nonlinear fashion between −5 and −25°C rather than between −20 and −40°C as in the simulation of natural clouds. Freezing of rainwater to graupel in natural clouds was assumed to proceed through a Bigg freezing process involving ice nuclei within the drops, while all rainwater in the AgI simulated cases was assumed to freeze between −5 and −10°C due to collisions with cloud ice particles (Orville and Hubbard, 1973). Salt seeding was simulated through changes in the parameters controlling autoconversion of cloud water to rainwater and by a shift toward larger raindrop sizes.

The AgI model predicts cloud tops (ACT) for AgI cases that are very close to MEH (Table 9). Table 9 also shows that, if both models are run on the same set of cases, the AgI version of the model predicts higher cloud tops than does the no-seed version. The significance of the difference in predictions has been tested by applying a rank-sum (Wilcoxon) test to the differences (MEH−NCT) and (MEH−ACT) for both classes of cases. For the no-seed cases a test statistic of −1.63 is found, significant at the 10% level (two-tailed test), but the test statistic of −1.12 for the AgI cases is significant at only the 26% level (two-tailed test). The former result tends to confirm the importance of simulating seeding treatments in modeling seeded clouds.

TABLE 9. Average errors and rank-sum test statistics for model predictions.*

	MEH−NCT (m)	Rank-sum test statistic	MEH−ACT (m)
No-seed cases	−230	← *−1.63* →	−790
	↑		↑
Rank-sum test statistic	*1.64*		*1.55*
	↓		↓
AgI cases	370	← *−1.12* →	−120

* Each rank-sum statistic (shown in italics) refers to comparison of two sets of numbers as indicated by arrows.

Further consideration of the test statistics in Table 9 shows that application of the no-seed model to the no-seed cases and the AgI version to the AgI cases provides optimum agreement between observations and model predictions. However, additional analyses of individual cases (not shown) showed no demonstrable skill at predicting which of the AgI cases would contribute the most to the indicated average height increase of 600 m.

e. Use of NCT as predictor of rainfall

The analysis with the aid of cloud models suggests that AgI seeding produced, on the average, height increases of the order of 600 m. Under the assumption that precipitation efficiency was not degraded as a result, this would lead to stimulation of precipitation and suggests that the analysis presented in Section 3, which used cloud depth as the indpendent variable, underestimated the total impact of AgI seeding. Therefore another covariance test has been applied to test

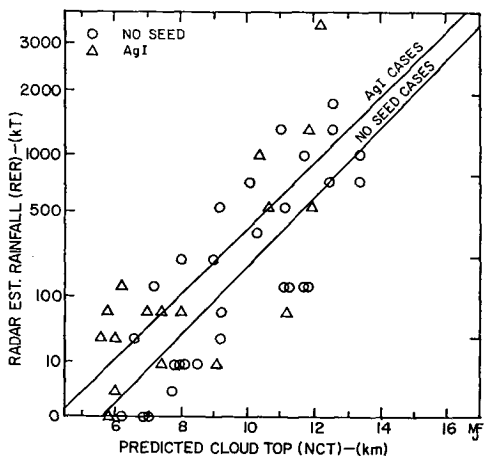

FIG. 7. Radar-estimated rainfall vs cloud top heights predicted by no-seed version of the model for no-seed and AgI test cases.

for differences between the silver iodide and no-seed cases, the dependent variable being the cube root of the radar-estimated rainfall (RER), and the independent variable being the cloud top (NCT) predicted by the no-seed version of the model (Fig. 7). The result is very similar to Fig. 4. For a given predicted cloud top height, more rain is indicated for the silver iodide cases than for the no-seed cases. The two regression lines are different at the 5% significance level, the difference being in the mean rainfall for the two classes. The slopes of the two lines are not significantly different.

5. Discussion

It would be an oversimplification to regard the apparent increases in shower extent and RER revealed by the covariance analysis of Section 3 as due solely to microphysical effects and the dynamic effects to be completely defined by the cloud model studies in Section 4. The variable RUP itself could be changed by dynamic invigoration of the largest cell in a test case. On the other hand, there could be dynamic effects not reflected in CDP, which was defined in terms of the maximum echo height (MEH) observed during each 1 h case. Much of the seeding was directed at new cloud towers forming around existing showers and seeding such towers could stimulate their growth without changing MEH or CDP.

As noted in Section 3b, the apparent effect of seeding brought out in the total analysis is not the addition of a tail of very light rain or virga to the natural rainfall rate distribution (Fig. 5). It is the addition (in space or time, or both) of shower areas resembling natural ones in intensity. As noted by perceptive observers over the years, the onset of precipitation in a convective cloud always affects its dynamics, which then affects the subsequent precipitation developments. It appears that cloud microphysics and cloud dynamics, including the influence of mesoscale wind fields around the clouds, must be considered together if the results of seeding experiments are to be fully understood.

6. Conclusions

For clouds of a given depth, the horizontal extent of shower areas and the radar-estimated rainfall during a 1 h test period were larger in cases seeded with either salt or silver iodide than in no-seed cases. Radar echoes were invariably observed in clouds of 2 km or greater depth following AgI seeding, while some unseeded and salt seeded clouds over 4 km deep failed to produce echoes. The observed differences are ascribed in part to the initiation of precipitation in newly developing cloud towers.

Comparison of maximum echo heights in silver iodide cases with those predicted by the no-seed version of a steady-state cloud model indicates increases in cloud height due to AgI seeding averaging about 600 m. The AgI version of the model predicts higher cloud tops than does the no-seed version of the model for both the no-seed cases and the AgI cases. Cloud tops predicted by the AgI version of the model on AgI cases and the no-seed version on no-seed cases are not statistically different from the observed values of maximum echo height in either class.

The project design took no account of possible interactions between the test cases and other clouds in the vicinity. Therefore, any indications of changes in rainfall associated with seeding in the Cloud Catcher experiment cannot be interpreted as changes in average rainfall over any large, fixed area incorporating the moving targets.

Acknowledgments. The research reported above was supported by the U. S. Department of the Interior, Bureau of Reclamation, Division of Atmospheric Water Resources Management, under Contract 14-06-D-6796 and was carried out under the general direction of Dr. Richard A. Schleusener. All computer calculations were carried out in the Computation Center of the South Dakota School of Mines and Technology.

The authors wish to pay tribute to Mr. G. A. P. Peterson, Mr. J. H. Boardman, and others who participated in the development of the computerized radar system used on the project. Dr. Harold D. Orville worked closely with us in the evolution of the cloud model. Thanks are extended to Miss Carol Vande Bossche and Mrs. Joie Robinson for work on the manuscript and to Mr. Melvin J. Flannagan for double duty as pilot and draftsman.

REFERENCES

Biswas, K. R., and A. S. Dennis, 1972: Calculations related to formation of a rain shower by salt seeding. *J. Appl. Meteor.*, **11**, 755–760.

Dennis, A. S., and A. Koscielski, 1972: Height and temperature of first echoes in unseeded and seeded convective clouds in South Dakota. *J. Appl. Meteor.*, **11**, 994–1000.

——, P. L. Smith, Jr., B. L. Davis, H. D. Orville, R. A. Schleusener, G. N. Johnson, J. H. Hirsch, D. E. Cain and A. Koscielski, 1974: Cloud seeding to enhance summer rainfall in the northern plains. Rept. 74-10, Inst. Atmos. Sci., South Dakota School of Mines and Technology, 161 pp. [Available at no cost from South Dakota School of Mines and Technology.]

Dixon, W. J., and F. J. Massey, Jr., 1957: *Introduction to Statistical Analysis*. McGraw-Hill, 488 pp.

Farley, R. D., and C. S. Chen, 1975: A detailed microphysical simulation of hygroscopic seeding. *J. Appl. Meteor.*, **14**, 718–733.

Hirsch, J. H., 1972: A numerical cloud model—Its use during Project Cloud Catcher. *Preprints Third Conf. Weather Modification*, Rapid City, S. D., Amer. Meteor. Soc., 182–185.

Hooke, R., and T. A. Jeeves, 1961: Direct search solution of numerical and statistical problems. *J. Assoc. Comput. Mach.*, **8**, 212–229.

Houghton, H. G., 1968: On precipitation mechanisms and their artificial modification. *J. Appl. Meteor.*, **7**, 851–859.

Orville, H. D., and K. G. Hubbard, 1973: On the freezing of liquid water in a cloud. *J. Appl. Meteor.*, **12**, 671–676.

Simpson, J., and A. S. Dennis, 1974: Cumulus clouds and their modification. *Weather and Climate Modification*, W. N. Hess, Ed., Wiley, 229–281.

Weinstein, A. I., and P. B. MacCready, Jr., 1969: An isolated cumulus cloud modification project. *J. Appl. Meteor.*, **8**, 936–947.